Rethinking the molecular $a_1(1420)$ and its partners in low lying axial-vector meson spectrum

严茂俊

In collaboration with J. Dias, A. Guevara, F.K. Guo and B.S. Zou

中国科学院理论物理研究所

April 27, 2024

Outline

Observations on $a_1(1420)$ in 3π final states

$\pi^- p \to \pi^-\pi^-\pi^+ p$ from COMPASS, F. Haas, Ph.D. thesis, Munich Tch. U. (2013)

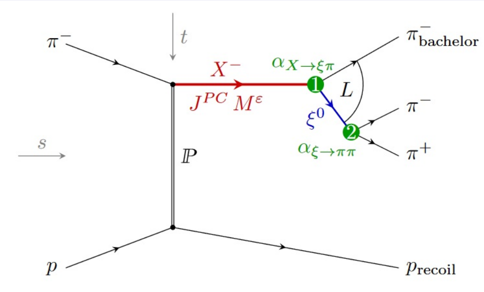

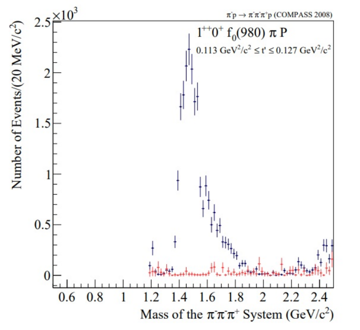

- Relativistic Breit-Wigner:

$$\mathcal{F}(m) = \frac{m_0\Gamma_0}{m_0^2 - m^2 - i m_0\Gamma(m)} \quad \text{with} \quad \Gamma(m) = \Gamma_0 \frac{m_0}{m}\frac{pF_L^2(p)}{p_0 F_L^2(p_0)}.$$

- $m = 1416, \quad \Gamma = 145\,\text{MeV}.$

$\pi^- p \to \pi^-\pi^-\pi^+ p$ from COMPASS, C. Adolph et al, PRL. 115 (2015) 8, 082001

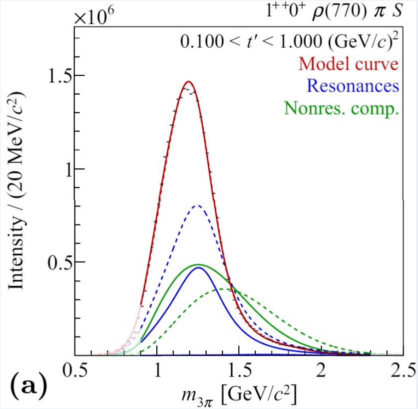

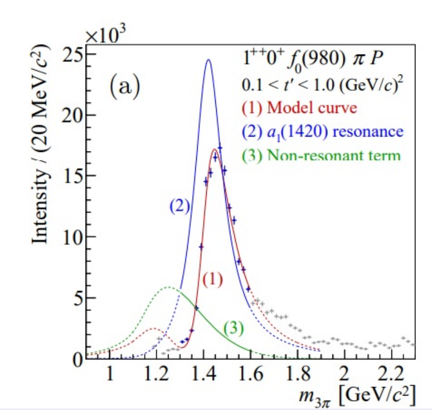

- $a_1(1420)$ mainly decays into $f_0(980)\pi$.
- mass $(1414^{+15}_{-13})\ \mathrm{MeV}$ and width $(153^{+8}_{-23})\ \mathrm{MeV}$.

Observations on $a_1(1420)$ in 3π final states

$\tau \to \pi^-\pi^-\pi^+\nu_\tau$ from Belle, Andrei Rabusov et al, HADRON2023

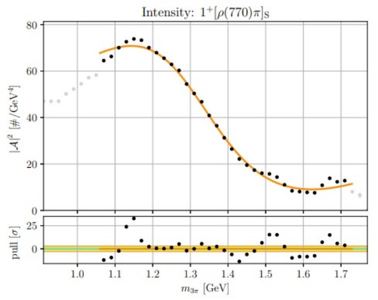

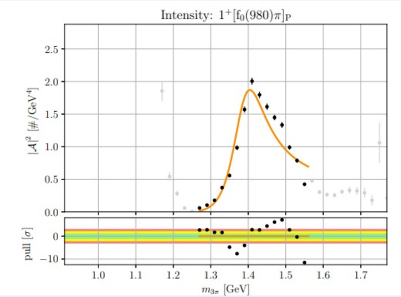

- $a_1(1260)$: (M,Γ) $=(1328.9 \pm 0.1, \quad 388.4 \pm 0.1)$.
- $a_1(1420)$: (M,Γ) $=(1387.8 \pm 0.3, \quad 109.2 \pm 0.6)$.

Hints on $b_1(1400)$ from BESIII in $J/\psi \to \phi\pi^0\eta$

Peak near $K^*\bar{K}$ threshold may couple to Z_s

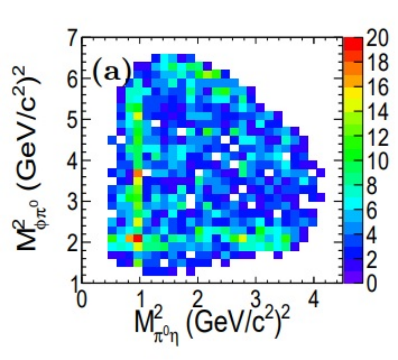

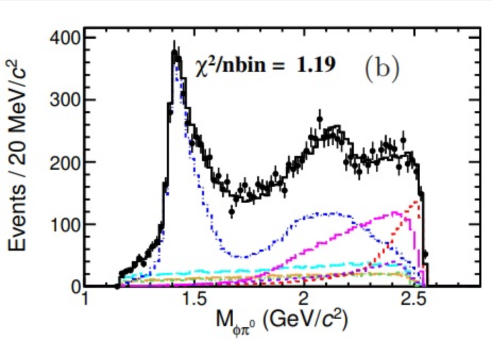

BESIII,PRL. 121(2018)2,022001,1802.00583; 2311.07043

The peak around 1400 MeV is non-ϕ background.

Models on $a_1(1420)$

- Tetraquark: H.X Chen et al, PRD 91 (2015), T. Gutsche et al, PRD 96 (2017) ;H. Sundu et al, PRD 97 (2018)
- Novelty: one pole generates two peaks in $\rho\pi - f_0(980)\pi$ scattering,Jean-Louis Basdevant et al, PPL. 114 (2015)
- Lattice: $a_1(1260)$ is $q\bar{q}$ and $a_1(1420)$ is not $q\bar{q}$,Y. Murakami et al, 1812.07765; $a_1(1260)$ is a dynamical pole of $\rho\pi$, M. Mai et al, PRL. 127 (2021);

- Tetraquark: H.X Chen et al, PRD 91 (2015), T. Gutsche et al, PRD 96 (2017) ;H. Sundu et al, PRD 97 (2018)
- Novelty: one pole generates two peaks in $\rho\pi - f_0(980)\pi$ scattering, Jean-Louis Basdevant et al, PPL. 114 (2015)
- Lattice: $a_1(1260)$ is $q\bar{q}$ and $a_1(1420)$ is not $q\bar{q}$, Y. Murakami et al, 1812.07765; $a_1(1260)$ is a dynamical pole of $\rho\pi$, M. Mai et al, PRL. 127 (2021);
- Triangle singularity: M. Mikhasenko et al, PRD 91 (2015); F. Aceti et al, PRD 94 (2016);G.D. Alexeev et al, PRL. 127 (2021)

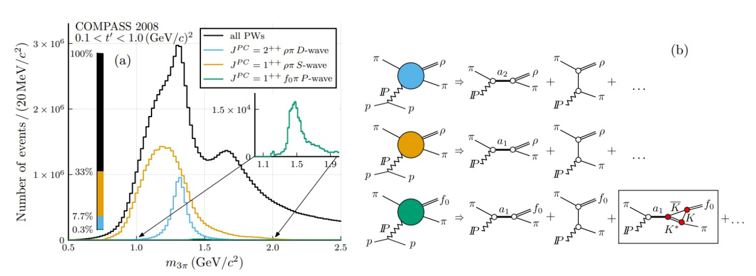

VP scattering in ChUA

Bethe-Salpeter equation

$$T = \left[1 + V\hat{G}\right]^{-1}(-V)\,\vec{\epsilon}\cdot\vec{\epsilon}',$$

with

$$\begin{aligned} V_{ij}(s) &= -\frac{\epsilon\cdot\epsilon'}{8f_\pi^2}C_{ij}\left[3s - \left(M^2 + m^2 + M'^2 + m'^2\right)\right. \\ &\left. -\frac{1}{s}\left(M^2 - m^2\right)\left(M'^2 - m'^2\right)\right]. \end{aligned}$$

VP scattering in ChUA

Bethe-Salpeter equation

$$T = \left[1 + V\hat{G}\right]^{-1} (-V)\,\vec{\epsilon}\cdot\vec{\epsilon}',$$

with

$$V_{ij}(s) = -\frac{\epsilon\cdot\epsilon'}{8f_\pi^2} C_{ij}\left[3s - \left(M^2 + m^2 + M'^2 + m'^2\right) - \frac{1}{s}\left(M^2 - m^2\right)\left(M'^2 - m'^2\right)\right].$$

On-shell approach in inelastic scattering

- $V_{ij}^{WT} \rightarrow V_{ij}^{WT}\frac{m_i}{E_{P_i}}\frac{M_i}{E_{V_i}}\frac{m_j}{E_{P_j}}\frac{M_j}{E_{V_j}},\ i \neq j$

UChA: C_{ij} of WT

	ϕK	ωK	ρK	$K^*\eta$	$K^*\pi$
ϕK	0	0	0	$-\sqrt{\frac{3}{2}}$	$-\sqrt{\frac{3}{2}}$
ωK	0	0	0	$\frac{\sqrt{3}}{2}$	$\frac{\sqrt{3}}{2}$
ρK	0	0	-2	$-\frac{3}{2}$	$\frac{1}{2}$
$K^*\eta$	$-\sqrt{\frac{3}{2}}$	$\frac{\sqrt{3}}{2}$	$-\frac{3}{2}$	0	0
$K^*\pi$	$-\sqrt{\frac{3}{2}}$	$\frac{\sqrt{3}}{2}$	$\frac{1}{2}$	0	-2

Table 2: C_{ij} coefficients in isospin base for $S=1$, $I=\frac{1}{2}$.

G		$\frac{1}{\sqrt{2}}(\bar{K}^*K+K^*\bar{K})$	$\phi\eta$	$\omega\eta$	$\rho\pi$	$\frac{1}{\sqrt{2}}(\bar{K}^*K-K^*\bar{K})$
$+$	$\frac{1}{\sqrt{2}}(\bar{K}^*K+K^*\bar{K})$	-3	0	0	0	0
$-$	$\phi\eta$	0	0	0	0	$\sqrt{6}$
$-$	$\omega\eta$	0	0	0	0	$-\sqrt{3}$
$-$	$\rho\pi$	0	0	0	-4	$\sqrt{3}$
$-$	$\frac{1}{\sqrt{2}}(\bar{K}^*K-K^*\bar{K})$	0	$\sqrt{6}$	$-\sqrt{3}$	$\sqrt{3}$	-3

Table 3: C_{ij} coefficients in isospin base for $S=0$, $I=0$. The first column indicates the

G		$\frac{1}{\sqrt{2}}(\bar{K}^*K+K^*\bar{K})$	$\phi\pi$	$\omega\pi$	$\rho\eta$	$\rho\pi$	$\frac{1}{\sqrt{2}}(\bar{K}^*K-K^*\bar{K})$
$+$	$\frac{1}{\sqrt{2}}(\bar{K}^*K+K^*\bar{K})$	-1	$-\sqrt{2}$	1	$\sqrt{3}$	0	0
$+$	$\phi\pi$	$-\sqrt{2}$	0	0	0	0	0
$+$	$\omega\pi$	1	0	0	0	0	0
$+$	$\rho\eta$	$\sqrt{3}$	0	0	0	0	0
$-$	$\rho\pi$	0	0	0	0	-2	$\sqrt{2}$
$-$	$\frac{1}{\sqrt{2}}(\bar{K}^*K-K^*\bar{K})$	0	0	0	0	$\sqrt{2}$	-1

Table 4: C_{ij} coefficients in isospin base for $S=0$, $I=1$. The first column indicates the

a_1 : $\rho\pi - K^*\bar{K}$ scattering in $I^G J^{PC} = 1^- 1^{++}$ sector

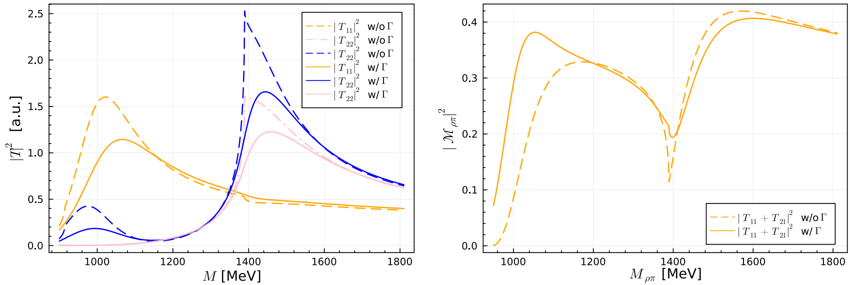

$q_{max} = 800$ and $1000\,\mathrm{MeV}$.
$z_r[\mathrm{MeV}] = 986.47 + i93.60\,(-+)$ and $1368.12 + i109.41(--)$.
Right: Inclusion of K^* width in evaluating T_{21}.

$K^*\bar{K} - f_0(980)\pi$ scattering in $I^G J^{PC} = 1^- 1^{++}$ sector

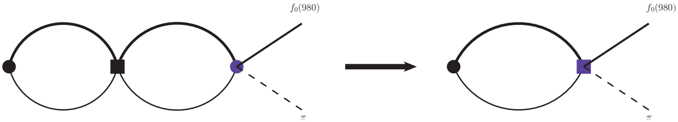

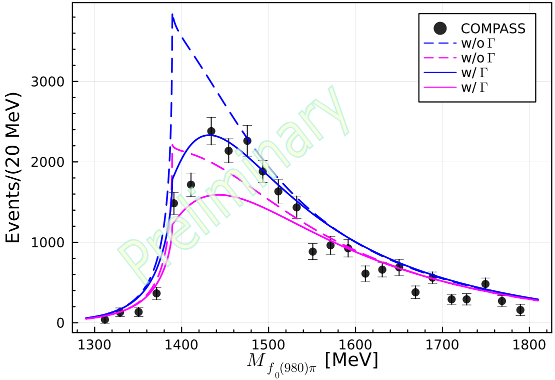

- $\mathcal{M} = V_p T_{K^*\bar{K},K^*\bar{K}}$, $\frac{dN}{dw} = |\mathcal{M}|^2 \frac{|\vec{k}_1|}{8\pi w}$

b_1 : $K^*\bar{K} - \phi\pi$ scattering in $I^G J^{PC} = 1^+1^{+-}$ sector

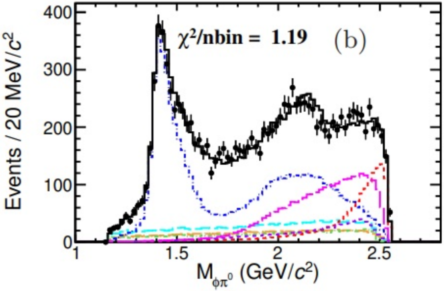

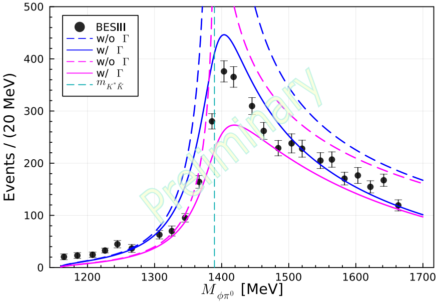

- Pole: $(1324.76 + i55.0)$ MeV
- $\mathcal{M} = V_p T_{K^*\bar{K},K^*\bar{K}}$, $\frac{dN}{dw} = |\mathcal{M}|^2 \frac{|\vec{k}_1|}{8\pi w}$
- $(M_R,\ \Gamma)$=(1380,91) A. Woss et al,PRD100(2019)5,054506

$\{\omega\pi, \phi\pi, \rho\eta, K^*\bar{K}\}$ scattering in $I^G J^{PC} = 1^+1^{+-}$ sector

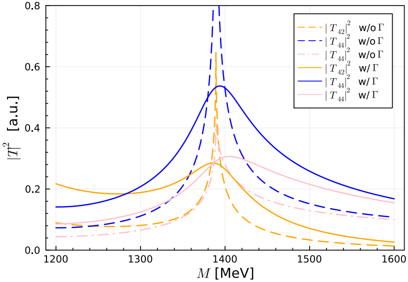

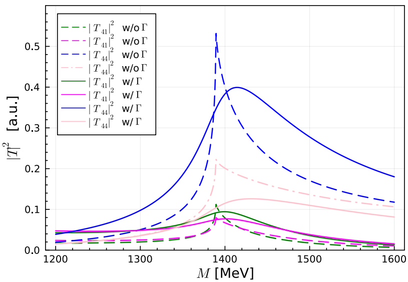

Peaks appear in $\phi\pi$ and $\omega\pi$ invariant mass distribution, the latter of which does not fulfill TS.

Isoscalar $|\bar{s}\bar{s}ud\rangle$ and K^*K scattering

T_{ss} in QCD sum rule and quark models

- $|\bar{s}\bar{s}ud\rangle$ predicted with mass from 1350 to 1600 MeV, Y. Cui et al, PRD73(2006);W.L. Wang et al,J.Phys.G34(2007);Q.X. Gao et al, J.Phys.G39(2012); .

T_{ss} in LO ChPT

- $|\bar{s}\bar{s}ud\rangle = \frac{1}{\sqrt{2}}\left|K^{*+}K^0\right\rangle - \frac{1}{\sqrt{2}}\left|K^{*0}K^+\right\rangle$, with $C_{ij}^{I=0} = 0$.

T_{ss} in LO ChPT and axial-vector meson exchange

- Axial-vector meson exchange: $\mathcal{L} = g_{a_1} a_{1,\mu} K^{*,\mu} \bar{K}$. M.J. Yan et al, PRD104(2021)
- $g_{a_1} \simeq \mathcal{O}(5000\,\mathrm{MeV})$, $V^{a_1} \simeq \mathcal{O}\left(\frac{g_{a_1}^2}{m_{a_1}^2}\right)$.
- $|V^{a_1}| \sim \left|V_{K^*\bar{K}}^{I=1}\right|/10$, too weak to bind.
- W/O additional dynamic, no T_{ss} around K^*K threshold.

Summary

- Besides the TS, there is a virtual pole in $K^*\bar{K}$ scattering in $I^G J^{PC} = 1^- 1^{++}$ sector.
- If $a_1(1420)$ were a molecular state, there is a dip in $\rho\pi$ invariant mass distribution that differes from TS.
- The peak in $\phi\pi$ invariant mass distribution could be a $b_1(1400)$ that generates a peak in $\omega\pi$ invariant mass distribution as well. This state is a flavor partner of $Z_c(3900)$.
- T_{ss} is hard to bind in isoscalar K^*K scattering.

- The near threshold virtual pole mainly determines the enhancement of lineshape.
- "Poles OR TS" to "Poles AND TS".

Summary

- Besides the TS, there is a virtual pole in $K^*\bar{K}$ scattering in $I^G J^{PC} = 1^- 1^{++}$ sector.
- If $a_1(1420)$ were a molecular state, there is a dip in $\rho\pi$ invariant mass distribution that differes from TS.
- The peak in $\phi\pi$ invariant mass distribution could be a $b_1(1400)$ that generates a peak in $\omega\pi$ invariant mass distribution as well. This state is a flavor partner of $Z_c(3900)$.
- T_{ss} is hard to bind in isoscalar K^*K scattering.

- The near threshold virtual pole mainly determines the enhancement of lineshape.
- "Poles OR TS" to "Poles AND TS".

Thanks !

Backup: $K^*\bar{K}$ scattering in $I^G J^{PC} = 1^- 1^{++}$ sector

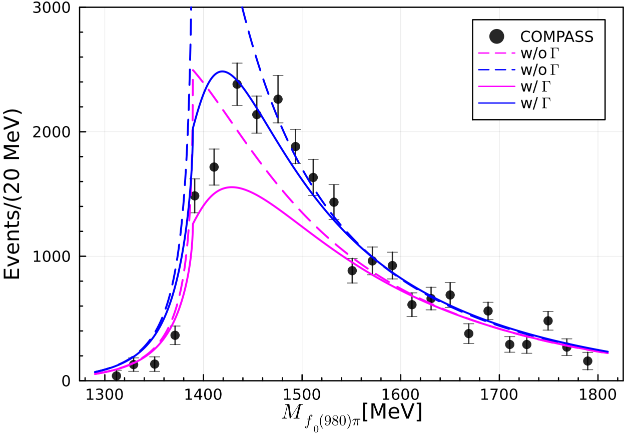

In the single channel scattering W/O modification on V_{ij},
$P_{a_1} = 346.41\,\mathrm{MeV}^{1/2}$.

Backup: $K^*\bar{K}$ scattering in $I^G J^{PC} = 0^+1^{++}$ sector

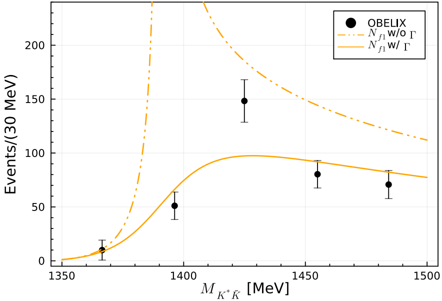

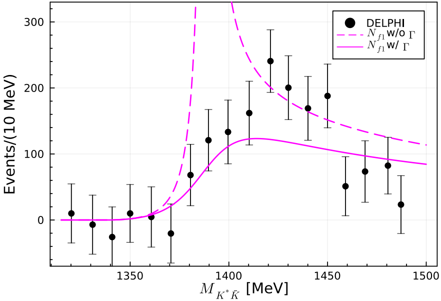

$$\mathcal{M}_{f_1} = \mathring{P}^{f_1}_{K^*\bar{K}} + \mathring{P}^{f_1}_{K^*\bar{K}}\, \tilde{G}_{K^*\bar{K}}\, T_{f_1} = P^{f_1}_{K^*\bar{K}}\, \tilde{G}_{K^*\bar{K}}\, T_{f_1},$$

$$\frac{dN_{f_1}}{dM_{K^*\bar{K}}} = \left|\mathcal{M}_{f_1}\right|^2 \frac{\left|\vec{k}_{K^*}\right|}{8\pi M_{K^*\bar{K}}}.$$

Backup: $\{\rho\pi, \omega\eta, K^*\bar{K}, \phi\eta\}$ scattering in h_1 spectrum

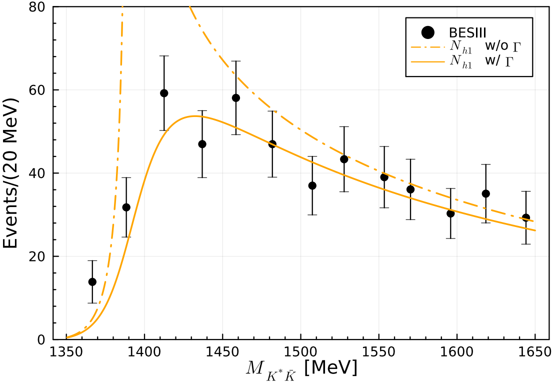

$$\mathcal{M}_{h_1} = \overset{\circ}{P}{}^{h_1}_{K^*\bar{K}} + \overset{\circ}{P}{}^{h_1}_{K^*\bar{K}}\, \tilde{G}_{K^*\bar{K}}\, T_{h_1} = P^{h_1}_{K^*\bar{K}}\, \tilde{G}_{K^*\bar{K}}\, T_{h_1}.$$

$$\frac{dN_{h_1}}{dM_{K^*\bar{K}}} = \left|\mathcal{M}_{h_1}\right|^2 \frac{\left|\vec{k}_{K^*}\right|}{8\pi M_{K^*\bar{K}}}.$$

Backup: $\{K^*\pi, \rho K\}$ scattering in $IJ^P = \frac{1}{2}1^+$ sector

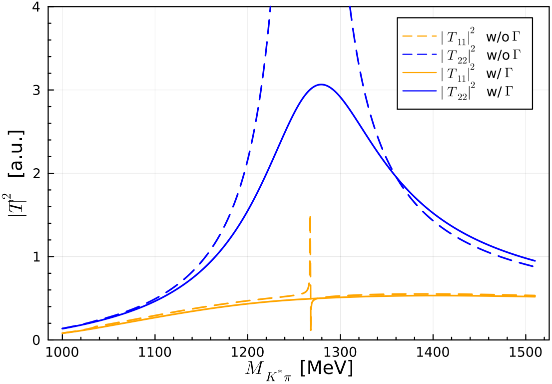

The lower pole is much smaller than the higher one in $|T_{ii}|$.

Backup: Left-hand-cut in $f_1(1285)$ spectrum

$$\tilde{V}^S_\eta = \frac{g_\eta^2 m_\eta^2}{4|\vec{q}|^2} \mathrm{Log}\left[\frac{u-2\vec{q}^2}{u+2\vec{q}^2}\right] = \frac{g_\eta^2 m_\eta^2}{4|\vec{q}|^2} \mathrm{Log}\left[\frac{\Delta\tilde{u}}{\Delta u}\right]$$